Journal of Cleaner Production 196 (2018) 1644–1656

Contents lists available at ScienceDirect

Journal of Cleaner Production

journal homepage: www.elsevier.com/locate/jclepro

Utilization of renewable waste material for the sustainable development of thermally stable and biologically active aliphatic amine modified Cardanol (phenolic lipid) - Formaldehyde free standing films

Shabnam Khan [a, 1], Shumaila Masood [a], Kehkashan Siddiqui [b], Manawwer Alam [c], Fahmina Zafar [a, **, 1], Qazi Mohd Rizwanul Haque [b], Nahid Nishat [a, *]

[a] Inorganic Materials Research Laboratory, Department of Chemistry, Jamia Millia Islamia, New Delhi 110025, India
[b] Microbiology Research Laboratory, Department of Biosciences, Jamia Millia Islamia, New Delhi 110025, India
[c] Research Centre-College of Science, King Saud University, P. O. Box 2455, Riyadh 11451, Saudi Arabia

ARTICLE INFO

Article history:
Received 27 November 2017
Received in revised form
7 June 2018
Accepted 9 June 2018
Available online 9 June 2018

Keywords:
Renewable resource
CNSL
Cardanol
Sustainable
Thermally stable
Antibacterial

ABSTRACT

The recognition of the alarming increased cost and looming exhaustion of petroleum resources for the production of polymeric resins for versatile applications has prompted us to switch towards green and sustainable resources. There is an immediate urge to develop bio-based polymeric resins via sustainable routes with enhanced properties for their utilization in polymer and coating applications. The present investigation reports the synthesis and characterization of aliphatic amine, Hexamethylene tetramine (HMTA) modified Cardanol(Col)-Formaldehyde(F) (Col-FA) free standing films and coatings for versatile applications through the use of cost-effective and renewable starting material, Col (agro byproduct of cashew nut processing) and HMTA (optimum amount, 15%) obviating the toxic solvent usage. The result indicated transparent (red-yellow colored), homogenous Col-FA films with amorphous morphology, and can serve as an eco-friendly, thermally stable (up to 430–440 °C), chemically resistant (against various solvents), mechanically robust and biologically active (moderate activity) material. The overall synthesis strategy is environmentally benign, employs safer chemistry and is consistent with the principles of "Green Chemistry" (principles 1, 2, 3, 4, 5, 6, 7, 8, and 12). This is a highly desirable and excellent approach to develop free standing, transparent, flexible, thermally stable, chemically resistant and antibacterial thin films/coatings to increase the application of Col.

1. Introduction

During past few years, many efforts have been expended on the utilization of renewable resources due to the growing environmental concerns. Among the renewable resources, cashew nut shell liquid (CNSL), an agricultural waste obtained as a byproduct of the cashew industry is unique in polymer industry (Khan et al., 2016a; Balgude et al., 2016). CNSL contains a mixture of anacardic acid, cardanol (Col), cardol and 2-methylcardol which has meta-substituted unsaturated/saturated 15-C alkyl chain along with the reactive phenolic ring (Balgude et al., 2016).

Col, a natural alkylphenol, can be regarded as a versatile and valuable raw material for oligomer/polymer production such as epoxies (Balgude et al., 2017a), phenalkamines (Pathak and Rao, 2006), polyols (Balgude et al., 2017b), polyurethanes (Khan et al., 2016 b), polyureas (Wazarkar et al., 2017), benzoxazines (Puchot et al., 2016; Calo et al., 2007; Rao and Palanisamy, 2011), azo dyes (Gopalakrishnan et al., 2011), Schiff base (Raj et al., 2011; More et al., 2010), resoles (Liang et al., 2016), novolac (Natarajan and Murugavel, 2013) and many others. Besides the widespread use of Col in polymers synthesis, production of materials for various applications has been reported, such as adhesives (Shukla et al., 2015), plasticizers (Greco et al., 2010, 2017; Greco and Maffezzoli, 2016), surfactants (Wang et al., 2015a), anti-biofilm coatings

* Corresponding author.
** Corresponding author.
E-mail addresses: fahmzafar@gmail.com (F. Zafar), nishat_nchem08@yahoo.com (N. Nishat).
[1] Equal contribution.

https://doi.org/10.1016/j.jclepro.2018.06.081
0959-6526/

(Zafar et al., 2016), phenolic foams (Shukla et al., 2015), antioxidants (Feng et al., 2017), drug delievery (Lalitha et al., 2015), flame retardant materials (Ravichandran et al., 2011) and others.

Novolacs are acid catalyzed phenol-formaldehyde (F) resins that are used for various industrial materials such as binding material, coatings, adhesives, brake friction materials and so on (Knop and Pilato, 1985). Novolac preparation proceeds through condensation reaction between phenol and F in the mole ratio of less than unity, resulting into soluble and fusible linear low molecular weight resins. This novolac resin does not react further itself; hence, a curing agent like hexamethylenetetramine or methenamine (HMTA) has been usually used to produce cross-linked materials (Wang et al., 2015b). The obtained novolac cured material has multiple advantages for application which needs quick curing, better mechanical properties and heat resistance. However, there has been a prodigious need for the design of environmental-benign pathways with the use of eco-friendly, cheap and non-toxic starting precursor, in accordance with green chemistry principles to produce the cleaner products. The replacement of phenol with Col for Col-F resin or novolac preparation can solve our concern to reduce the dependence on petroleum feedstock as well as improved properties of the developed novolac materials.

Previous studies revealed the synthesis of Col-F novolac resin for reinforcement of natural rubber (Chuayjuljit et al., 2007), semi-interpenetrating polymer network using Col-F (both resol and novolac resin) and polymethyl methacrylate (Manjula et al., 1991), Col based epoxidized novolac network blended with carboxyl-terminated butadiene acrylonitrile copolymer, further cured with stoichiometric amount of polyamine (Yadav and Srivastava, 2009), and Col-furfural based novolac resin cured with HMTA (Srivastava and Srivastava, 2013).

Literature survey indicated that a lot of research has been done to investigate the curing behavior of phenolic resins (usually petro-based) with HMTA (Wang et al., 2015; Medeiros et al., 2003) and modifications of Col-F. But to the best of our knowledge, no work is reported on the synthesis of aliphatic amine (HMTA) modified Col-FA thin film and coatings aiming towards green and sustainable chemistry that leads to the development of non-toxic and cleaner products with enhanced applications in different fields.

The primary objective in the present work is focused on the synthesis of aliphatic amine modified Col-FA free standing, transparent, flexible thin films via following “Green” chemistry principles. In this research, a cost-effective and environmental-friendly approach is utilized for the *in-situ* synthesis of Col-FA with further application in the development of thermally stable, chemical-resistant free standing films as well as mechanically-robust coatings for surface coating applications. The structure of the synthesized Col-FA was established with the aid of Fourier transform infrared spectroscopy (FTIR) and Nuclear magnetic resonance (^{1}H-NMR & ^{13}C-NMR) technique. The mode of Col-FA thin film formation was first time analyzed by FTIR - Attenuated Total Reflectance (ATR) spectral techniques and Differential Scanning Calorimetry (DSC). This work investigates the changes in opacity and color properties of the films with change in HMTA concentration. The effect of HMTA concentration on physico-mechanical behavior of coatings was also studied. The morphology was investigated using Field Emission-Scanning Electron Microscopy (FE-SEM) and X-ray diffraction (XRD) techniques. Thermogravimetric analysis (TGA)/Differential thermal analysis (DTA) was used to investigate the thermal stability of the prepared films. Chemical resistance of films was also investigated in 3.5% acid, base, neutral and salt medium to check their resistance towards chemicals. For preliminary antibacterial activity, Kirby Bauer disk-diffusion method was used to assess the activity of Col, Col-F and Col-FA resins against gram positive [*Staphylococcus aureus (S. aureus)*MTCC 902 and *Bacillus subtilis (B. subtilis)* MTCC 736] and gram negative bacteria [*Escherichia coli (E. coli)* MTCC 443 and *Pseudomonas aeruginosa (P. aeruginosa)* MTCC 2453].

2. Materials and methods

2.1. Materials

Col (Mol wt. 298.46 g/mol) (Golden Cashew Products Pvt. Lt. Pondicherry, India), [Specification: Color: gardeners standard 10; Specific gravity at 30 °C, 0.9268; viscosity at 30 °C, 47; iodine value, 235 and Mol. Mass - 298.46 g/mol]. F (37% w/v) [mol. wt. 30.03 g/mol, Merck specialities Pvt. Ltd. Mumbai], citric acid (anhyd.) [mol. wt. 192.13 g/mol, High Purity Laboratory Chemicals, Mumbai], HMTA [mol. wt 140.19 g/mol, Merck Limited, Mumbai], methanol [Loba Chemie Pvt, Ltd. Mumbai] and xylene [Merck Limited, Mumbai].

2.2. Synthesis of Cardanol-Formaldehyde (Col-F)

Col-F in the mole ratio 1:0.7 was prepared using citric acid as a catalyst by following the method published in our earlier work (Khan et al., 2016 b). Col (1 mol) was taken in a 250 ml three-necked round bottom flask. 0.7 mol of F was taken in a 50 ml beaker. Then the catalyst (1% based on Col) was dissolved in methanol at 60 °C in another beaker. Half of the catalyst solution was added to Col, charged in a three-necked round bottom flask fitted with a condenser and mechanical stirrer at 100 ± 5 °C. The remaining half of the methanolic solution of the catalyst was added to F and this was filled in burette and was added to reaction mixture drop wise within 1 h, and the temperature of the reaction kettle was maintained at 120 ± 5 °C. The reaction was carried out till pH of the reaction was dropped to 4 from initial pH of 6.5. Then the stirring was stopped and the content of the three-necked round bottom flask was transferred to a beaker. Col-F thus produced was a dark brown viscous liquid. The progress of the reaction was checked periodically with the help of TLC, pH and finally confirmed by FTIR. (Yield = 79.36%).

2.3. Synthesis of aliphatic amine modified Col-F (Col-FA)

For Col-FA resin synthesis, Col-F was taken in a 100 ml three-necked round bottom flask fitted with an air condenser and mechanical stirrer. It was kept on constant stirring in an oil bath till the temperature reached 120 ± 5 °C and kept for 30 min at this temperature. Then reaction temperature was reduced to 80±5 °C and subsequently maintained. At this temperature methanolic solution of HMTA (5%, 10%, 15%, 20% and 30% with respect to Col-F) was added slowly over the period of 15 min by using burette with continuous stirring. After complete addition of HMTA the temperature was raised and maintained at 100 ± 5 °C. The reaction was monitored periodically by TLC and FTIR. Sample designation and reaction condition for synthesis of Col-FA is given in Table 1. (Yield = 90–95%).

2.4. Preparation of Col-FA free standing thin films and coatings

To obtain the free standing thin films of all the compositions, Col-FA05 to Col-FA30, desired amount of material (70% by weight solution) was dissolved in xylene and poured onto Teflon sheets. They were then kept undisturbed at ambient temperature (28–30 °C) for 2 h and further at 80 °C for 30 min, followed by stepwise thermal curing at different temperature starting from 100 °C upto 180 °C for definite time period (listed in Table 2) to achieve the free standing films with desirable performance. After

Table 1
Sample designation and reaction condition for synthesis of Col-FA.

Code	Col: F (mole ratio)	HMTA (%)	Reaction time (min)	Reaction temperature (°C)
Col-FA05	1:0.7	05	15	100 ± 5
Col-FA10	1:0.7	10	15	100 ± 5
Col-FA15	1:0.7	15	15	100 ± 5
Col-FA20	1:0.7	20	20	100 ± 5
Col-FA30	1:0.7	30	60	100 ± 5

Table 2
The film formation schedule of Col-FA.

Temperature	Resin code				
	Time (hrs)				
	Col-FA05	Col-FA10	Col-FA15	Col-FA20	Col-FA30[a]
100 °C	2	2	2	2	2
120 °C	2	2	2	2	2
140 °C	2	2	2	2	2
160 °C	2	2	2	2	2
180 °C	2	2	2	2+2+2	2+2+2+2+2

[a] Did not form free standing film.

completion of curing they were allowed to cool at room temperature and these films were cut into appropriate dimension to be used for further analysis.

The commercially available carbon steel (CS) strips, having composition (in weight %) 2.87% C and 97.13% Fe, were employed for the preparation of Col-FA coatings. Prior to the coating preparation, the CS were successively polished with different grades of silicon carbide papers, thoroughly washed with double distilled water, degreased with methanol and acetone, and dried at room temperature. Col-FA05 to Col-FA 20 compositions (70% by weight solution in xylene) were applied using brush technique on CS of standard size (70 mm × 25 mm × 1 mm) for physico-mechanical testing. The CS were dried at room temperature for several hours, followed by stepwise drying from 100 °C to 180 °C for definite time period (same as discussed in the preparation of free standing films, Table 2).

2.5. Characterization of materials

Solubility of these materials were tested in various polar and non-polar solvents by taking 50 mg of material in 10 ml of solvent (e.g. xylene, dimethylformamide, ethanol, methanol, ethyl methyl ketone) in a closed test tube and set aside for 24 h.

TLC method was used to monitor the progress of the reaction. It was carried out by standard laboratory method.

FTIR spectra were recorded in the mid operating range of 4000-500 cm^{-1} using IR Affinity-1 CE spectrometer (Shimadzu corporation analytical and measuring instrument division, Kyoto, Japan). The samples were applied between two Zinc Selenide windows with a 0.05 mm thick teflon spacer. All the FTIR spectra were recorded averaging 40 scans with data spacing of 4 cm^{-1} and the data acquisition was achieved through IR solution software.

^{1}H-NMR and ^{13}C-NMR were performed on Bruker Avance III 500 MHz in deuterated chloroform ($CDCl_3$) using tetramethylsilane (TMS) as an internal standard.

ATR spectra of the cured films were recorded using Attenuated Total Reflectance (ATR, TENSOR 37 spectrophotometer, Germany) in the mid operating range of 4000-600 cm^{-1} by placing films onto the Universal Diamond ATR top plate and data acquisition was carried out through Opus-Spectroscopic software.

The thickness of the films was measured by an Elcometer instrument (Model 345 NT; Elcometer Instruments, Manchester, UK).

The opacity of the films was determined by placing 10 mm × 20 mm film portions into the test cell of U-3900 UV spectrophotometer Model 212-0013 and using the empty cell as a reference. The opacity was calculated by measuring the absorbance at 650 nm following the method reported earlier (Wang et al., 2017; Peng et al., 2013) by using the equation:

$$O = Abs_{650} / d$$

where, O is the opacity, Abs_{650} is the absorbance value at 650 nm and d is the film thickness (mm).

The color of Col-FA films was evaluated using Gretag Macbeth Color-Eye 7000 A Spectrophotometer in terms of CIE Lab values (L^*, a^*, b^*, C^*, h and ΔE_{cmc}). Where, 'L*' denotes lightness based on a scale from black to white with grey in the middle, 'a*' measures redness (+ve) or greenness (-ve) and 'b*' measures yellowness (+ve) or blueness (-ve).

C^* (Chroma) represents the departure of color from grey, h (Hue) describes the overall color of an object, i.e., how much red, green, blue or yellow, ΔE_{cmc} defines elliptical color difference space around the product standard.

The physico-mechanical performance of the coatings was tested by analyzing the scratch hardness (BS 3900), impact resistance (IS: 101 part 5 s^{-1}, 3, 1988), bend test (1/8 inch conical mandrel, ASTM-D3281-84) and specular gloss at 45° by gloss meter (model RSPT 20; Digital Instrument, Santa Barbara, CA, USA). The adhesion of the coatings on the CS was evaluated using the crosshatch adhesion method (ASTM D 3359).

The wide angle powder XRD patterns of the materials were recorded using X-ray diffractometer (Ultima IV model, Rigaku cooperation, Japan) with Cu Ka radiation (k50.15406 nm). The spectra were recorded against 2θ from 10 to 60° with a scan rate of 1° min^{-1}. Optical microscope (Leitz, Wetzlar, Germany) was used to study the surface morphology of the materials.

FE-SEM Scanning Electron Microscope (model ZEIS EVO 50 SERIES) was used to analyze the morphology of the samples and its surface composition.

The thermal stability and film formation of Col-FA was studied by TGA/DTA and DSC, respectively [Mettler Toledo AG, Analytical CH-8603, Schwerzenbach, Switzerland] under nitrogen atmosphere at a heating rate of 10°C min^{-1}. Integral procedural decomposition temperature (IPDT) method as initially proposed by Doyle (1961) was calculated from TGA thermogram that correlates to the volatile parts of the polymeric material and is used to assess the inherent thermal stability of the polymeric materials (Vyazovkin and Sbirrazzuoli, 2006; Laxmi et al., 2018). IPDT accounts for the whole shape of the curve in a single number by measuring the area under the curve. In the present work, IPDT was calculated as follows:

$$IPDT(^{\circ}C) = A^{*}K^{*}\left(T_f - T_i\right) + T_i \quad (1)$$

$$A^* = S_1 + S_2/S_1 + S_2 + S_3 \quad (2)$$

$$K^* = S_1 + S_2/S_1 \quad (3)$$

Where, A^* is the area ratio of the total experimental curve defined by the total TGA thermogram, T_i is the initial experimental temperature, and T_f is the final experimental temperature. The representations of S_1, S_2, and S_3 for calculating A^* and K^* have been shown in many reported works on IPDT (Yadav et al., 2012).

Chemical resistance of films was checked using 3.5% solutions of acid, base and salt along with water by the following formula:

% Weight loss = [(Initial weight - Final weight)/Initial weight] X 100.

2.6. Antibacterial activity

Preliminary antibacterial activity of Col, Col-F and Col-FA was determined with respect to Ampicillin (as standard control drug) following Kirby Bauer disk-diffusion method against gram positive (*S.aureus*and *B. subtilis)* and gram negative bacteria (*E.coli,* and *P. aerugenosa)*. Mueller-Hinton agar (HiMedia India) plates were inoculated by 50 μl of 0.5 McFarland unit grown test organisms to get a uniform loan of culture. Circular wells of 6 mm diameter were made using sterile steel borer at appropriate distance and 10 μl Col, Col-F and Col-FA were added at a concentration of 62.5 mg/ml, 125 mg/ml and 187.5 mg/ml. The parafilm sealed plates were incubated at 37 °C for 12–14 h. After incubation, zone of growth inhibition (mm) presenting antimicrobial activity of test compounds was measured.

The bacterial cultures were procured form Microbial Type Culture Collection and Gene Bank, IMTECH Chandigarh, India, with the culture collection nos. - MTCC 443 (*E.coli*), MTCC 736 (*B.subtillis*), MTCC 902 (*S.aureus*) and MTCC 2453 (*P.aeruginosa*).

3. Results and discussion

3.1. Synthesis

Scheme 1 represents the chemical reactions involved in the synthesis of Col-FA from Col. It reveals the two major steps involved in the synthesis, synthesis of Col-F (Step I) and Col-FA (step II). Step I (synthesis of Col-F) carried out by condensation reaction between Col and F at 120 ± 5 °C in the presence of acidic catalyst to produce Col-F. This step results in the substitution of methylol group or $-CH_2OH$ at ortho position (Khan et al., 2016 b), which is confirmed by FTIR spectra discussed in Section 3.2. Step II (synthesis of Col-FA) carried out via two step *in situ* method. The synthesis involves the formation of ether linkage by condensation reaction between Col-F moieties with the removal of water molecule at 120 ± 5 °C in presence of acid followed by the amination reaction with HMTA at 100±5 °C. The latter reaction initiated with *in situ* synthesized water that is formed during the former reaction. HMTA break down *in situ* into formaldehyde and ammonia that react to form Col-FA (García et al., 2010). This step proceeds through the formation of most stable benzoxazine intermediate (Zhang and Solomon, 1998) in the present case among all the possible intermediates such as hydroxybenzylamine and benzoxazine discussed in detail in Section 3.2.

It was observed that both reactions (methylolation and amination) were carried out with the use of minimum possible solvent. In the present case, methanol (low boiling point) was used (minimum) during the synthesis that evaporated at high temperature. However, Col was effectively used as base material, reaction medium (provide functional group for the reaction) and reactive diluent to carry out these reactions **s**uccessfully due to long alkyl chain and reactive phenolic hydroxyl group that offers respectively, synthetic flexibility and functional sites for the synthesis (Zafar et al., 2016; Lochab and Varma, 2012). The overall reaction was carried out through environmental benign chemical route that is, it follows most of the principles of Green Chemistry (Anastas and Warner, 1998).

The solubility data clearly reveals that Col-FA was soluble in DMSO, THF, hexane, chloroform, xylene and ethyl methyl ketone while insoluble in common organic solvents such as water, ethanol, methanol even after 24 h.

3.2. Spectral analysis

Fig. 1.1 and 1.2 depicted FTIR spectrum of Col, Col-F, Col-FA (Col-FA05 to Col-FA 30). The following characteristic peaks were observed: **Col** (Zafar et al., 2016):3345 cm^{-1} (−OH υ, intermolecular hydrogen bonded), 3061 cm^{-1} (Ar C═C−H υ), 3007 cm^{-1} (C═C−H υ), 2931 and 2854 cm^{-1} (asymm and symm CH_2/CH_3 υ), 1589 cm^{-1} (C═C, υ), 1265 cm^{-1} and 1153 cm^{-1} (phenolic C−O υ), 1071 cm^{-1} (tert. C−OH, υ), and 782 cm^{-1} (C−H out of plane δ). **Col-F:** 3351 cm^{-1} (−OH υ, broad), 3076 cm^{-1} (Ar C═C−H υ), 3009 cm^{-1} (C═C−H υ), 2926 and 2855 cm^{-1} (asymm and symm CH_2/CH_3 υ), 1589 cm^{-1} (C═C υ), 1265 cm^{-1} and 1155 cm^{-1} (phenolic C−O υ), 1072 cm^{-1} (tert. C−OH. υ) and 1097 cm^{-1} (C−O υ of CH_2OH), 782 cm^{-1} (C−H out of plane δ) and 746 cm^{-1} (ortho substitution at benzene ring). **Col-FA:** 3062-3091 cm^{-1} (Ar C═C−H υ), 3008-3010 cm^{-1} (C═C−H υ), 2923-2927 cm^{-1} and 2852-2854 cm^{-1} (asymm and symm CH_2/CH_3 υ), 1580-1581 cm^{-1} (C═C υ), 1487-1504 cm^{-1} (tetrasubstituted benzene ring υ), 1350-1374 cm^{-1} (C−N υ), 1261-1275 cm^{-1} (phenolic C−O υ), 1240-1248 cm^{-1} (asymm. C−O−C υ in aryl alkyl ether), 1155-1165 cm^{-1} (C−N−C υ), 1114-1120 cm^{-1} (asymm. C−O−C υ in dialkyl ether), 1010-1020 cm^{-1} (symm. C−O−C υ) and 964-971 cm^{-1} (N−CH_2−O or N−C−O υ).

The FTIR spectra of Col-F is somewhat identical to Col with all the characteristic peak of Col alongwith some additional peaks as reported in our previous work (Khan et al., 2016 b). The FTIR spectra of Col-FA05, Col-FA10, Col-FA15, Col-FA20, Col-FA30 (Fig. 1.1c–1.2 a-d) reveals the gradual disappearance of −OH stretching peak at 3345-3351 cm^{-1} as percentage of HMTA increases from 5 to 30%. There is also disappearance of peak at 1072 and 1091 cm^{-1} due to tert. C−OH and primary C−OH υ, respectively, that can be correlated to the reaction between two methylol group in Col-F resulting in the formation of ether linkage as confirmed by the appearance of peak at 1114-1120 cm^{-1} typical of dialkyl ether linkage. This formation is followed by the amination reaction of available phenolic −OH group with amine group of HMTA leading to the formation of most stable benzoxazine intermediate in our case (Zhang and Solomon, 1998). The FTIR spectra of Col-FA showed significant bands at 1240-1248 cm^{-1} (asymmetric C−O−C), 1010-1020 cm^{-1} (symmetric C−O−C) (Rao and Palanisamy, 2011) and 964-971 cm^{-1} (N−CH_2−O or N−C−O) stretching (Vaithilingam et al., 2017), typical of benzoxazine ring structure except Col-FA05 in which all these peaks are much less intense. All the compositions of Col-FA showed some additional peaks in comparison to Col-F at 1487-1504 cm^{-1}, 1155-1165 cm^{-1} due to tetrasubstituted benzene ring υ (Velez-Herrera and Ishida, 2009) and C−N−C υ (Ishida and Ohba, 2005), respectively, which again confirm the involvement of benzoxazine type structure. It can also be seen that as the percentage of HMTA increases, the peak area and value due to tetrasubstituted aromatic ring increases upto 20%. Hence, the disappearance of O−H

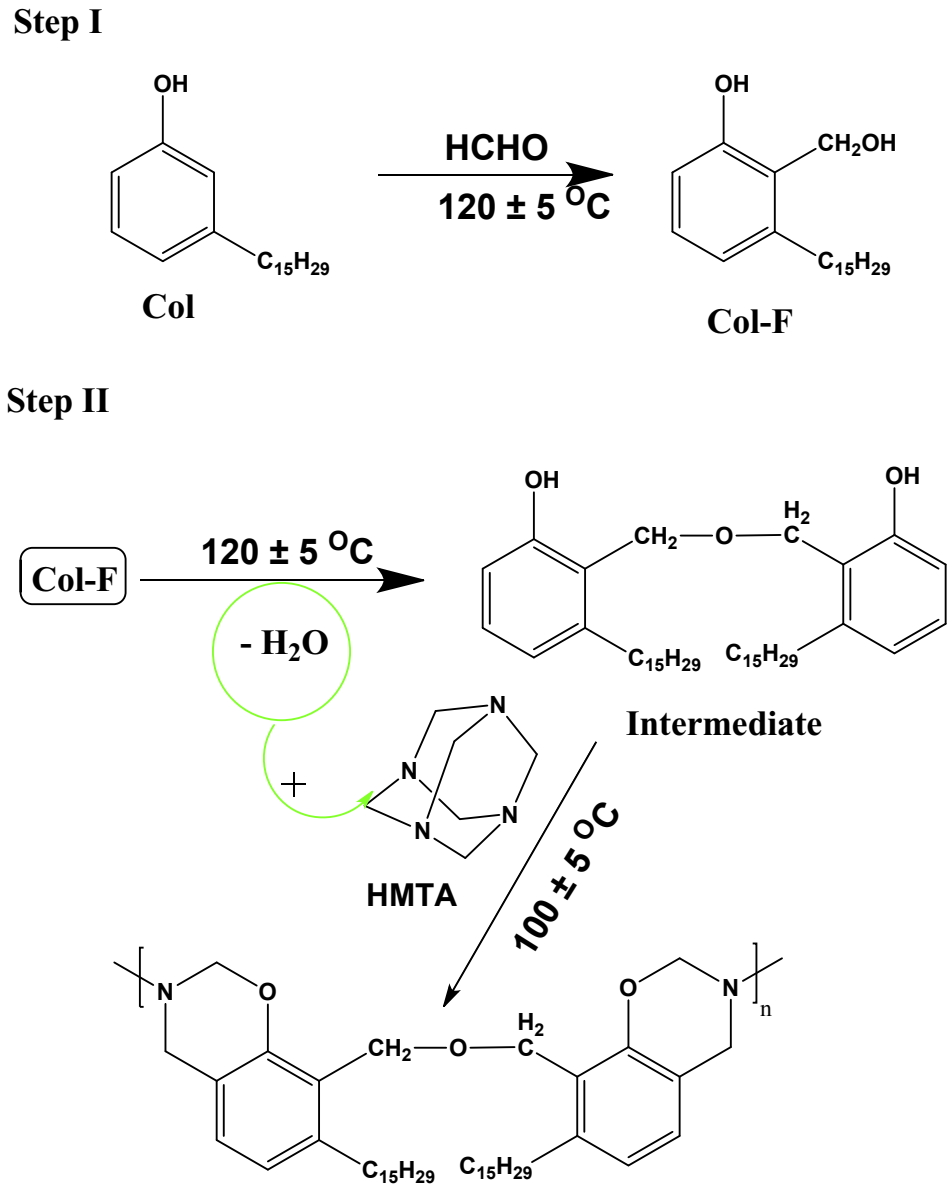

Scheme 1. Synthesis of Col-FA resin.

peak alongwith appearance of some additional peaks indicates utilization of Col and HMTA towards the formation of benzoxazine type ring structure as an intermediate. There is also appearance of peak at 1350-1374 cm^{-1} due to the C–N υ that can further be correlated to the presence of nitrogen-containing functional groups as an intermediate in Col-FA (Vaithilingam et al., 2017). It is also observed that C–N υ peak becomes more pronounced with increasing content of HMTA from 5 to 30% indicating the involvement of mainly nitrogen-containing species.

3.3. NMR spectral analysis

^{1}H-NMR (Fig. 2.1) and ^{13}C-NMR (Fig. 2.2) spectral analysis of Col-FA15 shows the following characteristic peaks:

Col-FA15, ^{1}H-NMR ($CDCl_3$, 500 MHz, δ ppm**):** 0.99 (C**H**$_3$/C**H**$_2$, l), 1.15–1.41 (chain –C**H**$_2$-, f), 1.68 (C**H**$_2$–CH_2–Ar, e), 2.13–2.26 (C**H**$_2$–CH=CH, g), 2.63 (C**H**$_2$-Ar, d), 2.89 (CH=CH–C**H**$_2$–CH=CH–, i), 4.06–4.10 (–ArC**H**$_2$–O–C**H**$_2$-, c), 4.76 (Ar–C**H**$_2$–N–, m), 4.9 (–O–C**H**$_2$–N–, n), 5.06–5.12 (CH=C**H**$_2$, k), 5.45–5.51 (C**H**=C**H**, h), 5.89 (C**H**=CH_2, j), and 6.62–7.16 (Ar–**H**, a, b).

^{13}C-NMR ($CDCl_3$, 500 MHz, δ ppm**):** 13.94–14.27 (**C**H_3, t), 22.92–29.88 (chain –**C**H_2–, j), 31.46–36.03 (–CH=CH–**C**H_2–, k,n,q), 47.12–54.63 (Ar–**C**H$_2$–N–, u), 74.14 (Ar–**C**H$_2$–O–CH_2–, g), 80.70 (–N–**C**H_2–O–, v), 112.79–129.93 (**C**H=**C**H, **C**H=CH_2, CH=**C**H_2, l, m, o, p, r, s), 130.01–136.84 (Ar**C**, b, c, d, f), 143.29–144.73 (Ar**C**-R, e), and 153.2–157.41 (Ar**C**–O–, a).

On comparing the ^{1}H-NMR and ^{13}C-NMR of Col-FA15 with the spectra of Col, as reported in our earlier published work (Zafar et al., 2016), the appearance/disappearance of certain peaks is evident confirming the structure of Col-FA. Fig. 2.1 shows the ^{1}H-NMR of Col-FA with the same characteristic protons of aliphatic alkyl chain in the range of 0.99–2.89 and 5.06–5.89 ppm. The aromatic ring

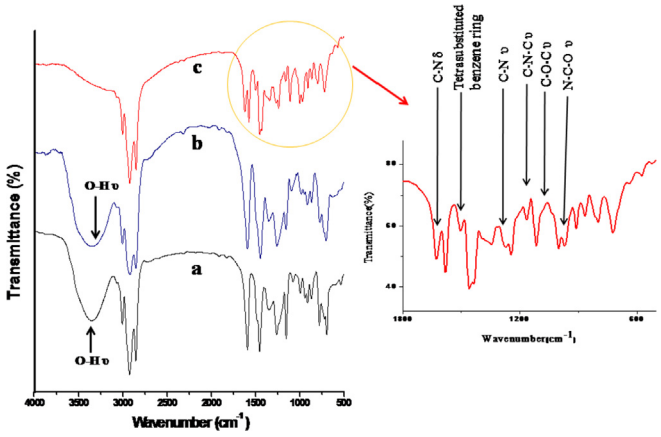

Fig. 1.1. FTIR spectra of (a) Col (b) Col-F (c) Col-FA15.

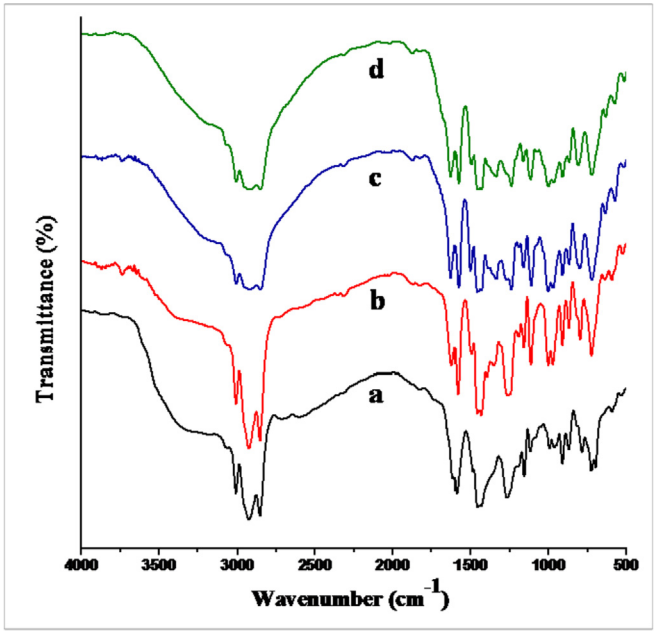

Fig. 1.2. FTIR spectra of (a) Col-FA05 (b) Col-FA10 (c) Col-FA20 and (d) Col-FA30.

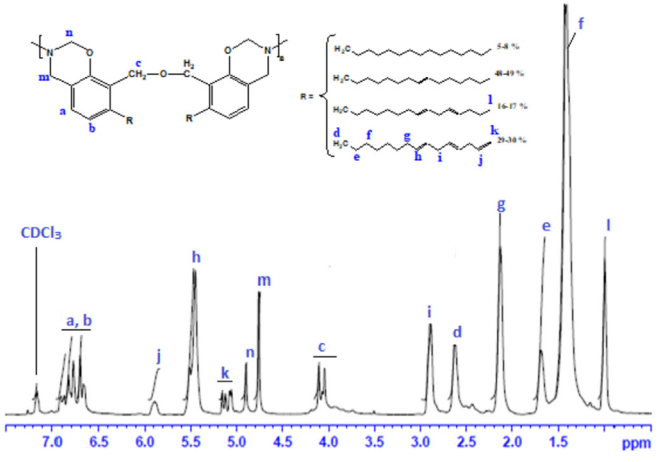

Fig. 2.1. ^{1}H-NMR spectra of Col-FA15.

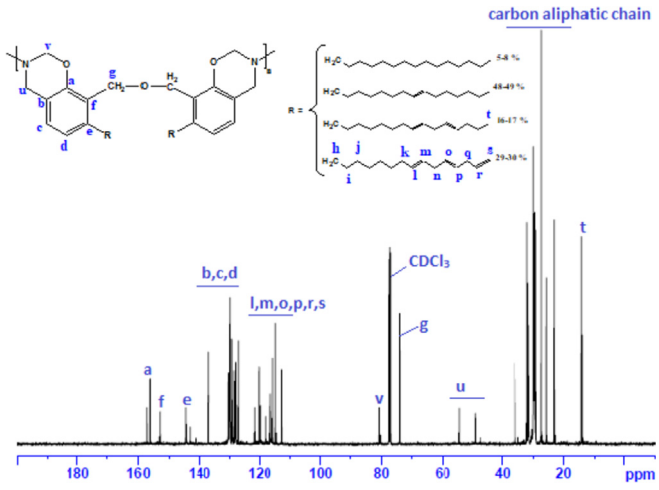

Fig. 2.2. ^{13}C-NMR spectra of Col-FA15.

protons appeared as multiplets between 6.62 and 7.16 ppm. The ^{1}H-NMR spectra revealed the disappearance of ArC—OH peak as compared to Col indicating its possible involvement in benzoxazine ring formation. The characteristic protons of oxazine ring are observed at 4.76 and 4.9 ppm (Ar—C**H**$_2$—N— and —O—C**H**$_2$—N—) (Li and Yan, 2015), respectively. In addition to this, a new peak observed at 4.06–4.10 ppm that corresponds to -CH$_2$— of ether linkage (—ArC**H**$_2$-O—C**H**$_2$-, c) with a downfield shift due to the aromatic ring.

Fig. 2.2 shows the ^{13}C-NMR spectra of Col-FA15 in which the characteristic oxazine ring carbon resonances at 47.12–54.63 and 80.70 ppm for Ar—**C**H$_2$—N— and —N—**C**H$_2$—O—, respectively, further confirming the Col-FA structure. The peak at 74 ppm corresponds to the —**C**H$_2$— of ether linkage. The NMR spectral result thus also confirms the proposed structure of Col-FA as reported in Scheme 1 (Silverstein et al., 1991).

3.4. Thin films formation

For the preparation of thin film, Col-FA was kept in vacuum oven at 180 °C for 1–2 h. However, pores and cracks were observed on the whole surface of Col-FA film. Therefore, we have to optimize the curing temperature and time for the preparation of Col-FA thin films for various applications. Table 2 shows the optimized curing temperature and time for the preparation of Col-FA thin film. It is clear from the cure schedule that Col-FA20 thin film formation take longer time as compared to Col-FA05, Col-FA10 and Col-FA15 at 180 °C. In addition, the composition Col-FA30 did not cured properly to form free standing film even after prolonged heating. Hence, the obtained free standing thin films of only four different compositions (Col-FA05, Col-FA10, Col-FA15 and Col-FA20), reddish-yellow in color and transparent in nature according to the mentioned curing steps. There were no bubbles and cracks on the surface of Col-FA films. These obtained thin films were flexible and can be bent as shown in Fig. 4b. The flexibility of the film is due to long aliphatic alkyl chain present in the Col-FA that imparts flexibility (Sharmin et al., 2016).

The film formation of Col-FA (Fig. 3) proceeds through two step processes i.e. physical and chemical. The physical process involves solvent evaporation along with polymer chain entanglement. The chemical (thermally activated) process involves the complex reactions of available functional groups at elevated temperature. This film forming ability of Col-FA was confirmed by using ATR-FTIR (Fig. 5) of cured films and compared with the FTIR of uncured

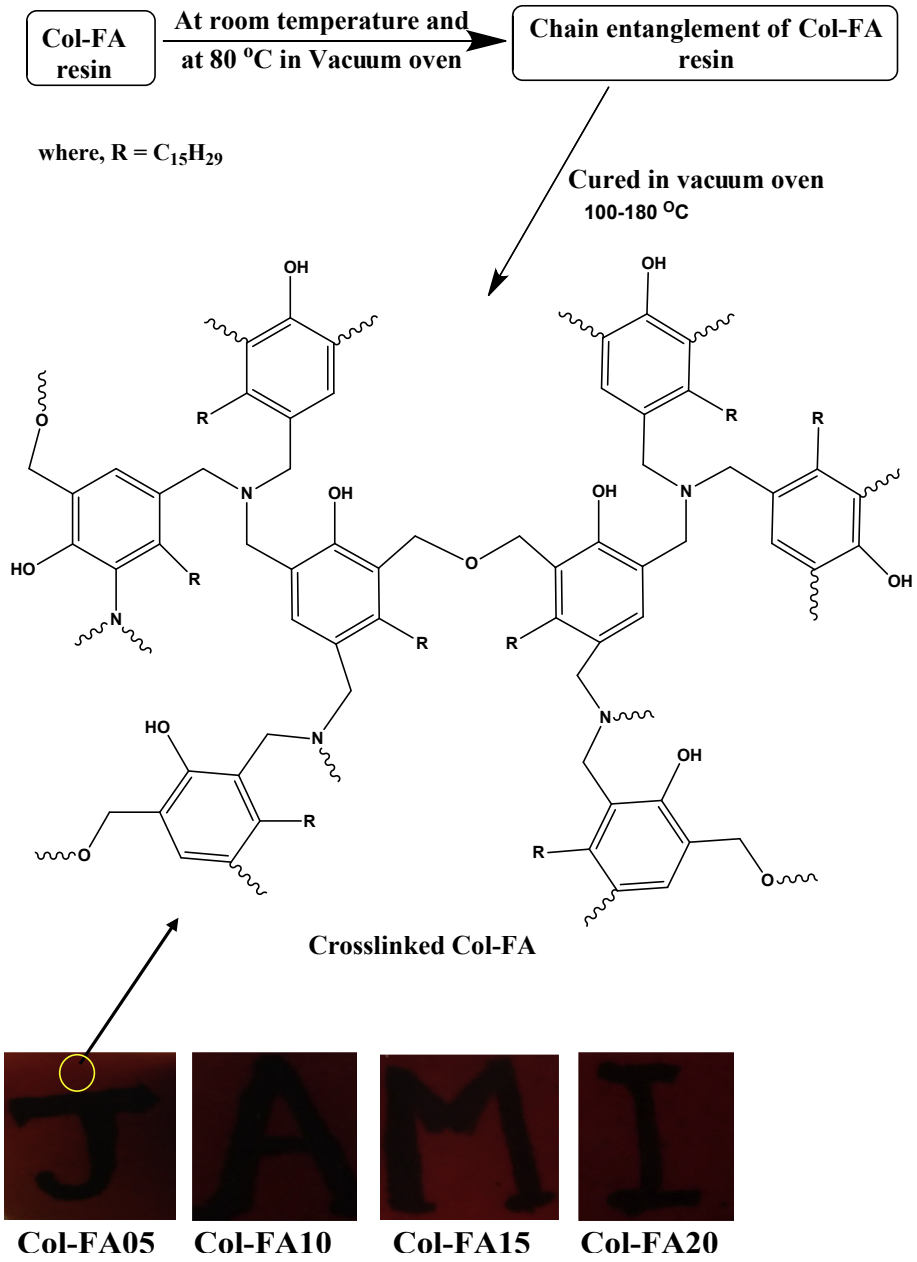

Fig. 3. Col-FA thin film formation.

samples of Col-FA. The ATR-FTIR spectrum reveals the re-appearance of broad peak due to phenolic -OH υ at 3360-3364 cm^{-1} and decrease in intensity of peak at 1349-1365 cm^{-1} (C–N υ) that can be corroborated to the presence of N-alkylated moieties in Col-FA thin films. The ATR spectra also depict the disappearance of characteristic peaks of benzoxazine (964-971 cm^{-1}) (Vaithilingam et al., 2017) and tetrasubstituted benzene ring (1487-1504 cm^{-1}) in Col-FA10 to Col-FA20. However, in Col-FA05 the above mentioned peaks were present with much less intensity. Hence, the aforementioned results can be correlated to thermally-induced benzoxazine ring opening leading to cross-linked structure of Col-FA thin films (Zhang and Solomon, 1998). These results were further confirmed with the help of DSC technique.

In DSC thermogram (Fig. 6a–d), a small endothermic peak centered at 43 °C in Col-FA05, while at 59–60 °C in Col-FA10, Col-FA15 and Col-FA20 corresponds to their melting temperatures (Li and Yan, 2015). This endothermic peak followed by a very broad endotherm ranging from 65 °C - 190 °C, 65 °C - 210 °C, 65 °C –215 °C, respectively for Col-FA10, Col-FA15 and Col-FA20 except Col-FA05, that can be correlated with molecular rearrangement or removal of entrapped solvent. TGA also shows no weight loss at this temperature range. DSC also shows two exothermic peaks (small and big) ranging from 200 °C-290 °C and 290 °C-400 °C, respectively. The peaks maxima for Col-FA05 and Col-FA10 were observed at 248 °C, 342 °C whereas for Col-FA15 at 268 °C, 347 °C, and for Col-FA20 at 268 °C, 342 °C. TGA/DTA (Fig. 7.1–Fig. 7.4) also showed very slight weight loss at the temperature range 200–400 °C. Therefore, these exothermic behaviors at higher temperature region can be associated to the thermal-activated ring opening polymerization of oxazine rings (first maxima) of Col-FA(Li and Yan, 2015) followed by the cross linking

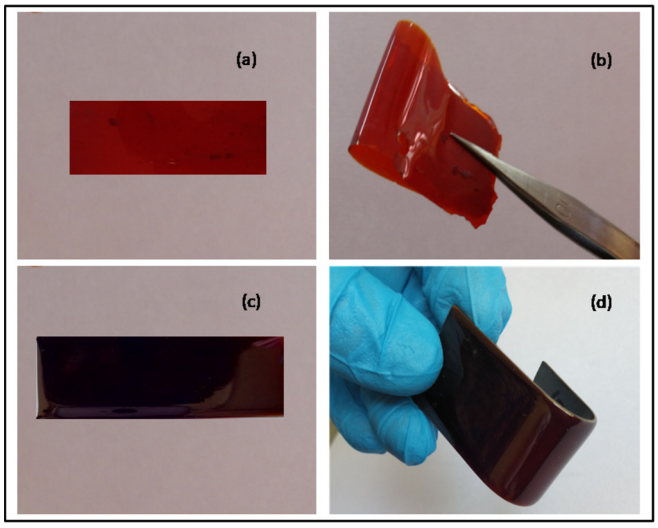

Fig. 4. Film (a) before bent and (b) after bent, and coating (c) before bent (d) after bent of Col-FA15.

(second maxima) of the polymeric chain by the removal of small molecules (like ammonia, formaldehyde) (Fig. 3).

3.5. Film appearance, thickness and opacity

The obtained Col-FA films were homogeneous, flexible and transparent as observed through naked eye observation (shown in Figs. 3 and 4b) that indicated the better compatibility among film components. If the compatibility among different constituents of films is not appreciable, then the opacity is high or transparency is low due to reflection or dispersion of light at phase interface (Martins et al., 2012). The thickness and opacity of the films at selected wavelength are listed in Table 3. From the results obtained, the thickness of the films showed no significant difference and was found to be in the range of 110–180 μm. The opacity values (listed in Table 3) indicated that with increasing HMTA concentration upto 10%, the opacity value of Col-FA also increased. However, the opacity value of Col-FA15 films was found to be low, suggesting it to be more transparent among all compositions.

3.6. Color properties of thin films

Color of the film is an important parameter in terms of general appearance and consumer acceptance. The visual color perception is purely subjective in nature and can be affected by outside factors such as lighting environment and material of the object. The different color models are available for the quantitative representation of color. Among them, CIELAB (CIELab) is the commonly used color space as it represents color the same way as humans perceive color and thus ideal for visual color matching.

Table 4 depicts the CIELab and CIELch values of Col-FA films with different % concentration of HMTA. It is clear from the data that on increasing the percentage of HMTA (10%–20%), there was a slight increase in L^* and decrease in C^* values indicating the light and bright shades of the films respectively (Rather et al., 2014). The positive values of a^* and b^* indicated the red and yellow tinge characteristics of the films and falls in the moderate red-yellow zone of CIE-Lab color space. With the increase in HMTA concentration, the values of overall color difference (ΔE_{cmc}) decreased that indicates less colored films. The decrease in h values, indicate redder color for the films with increased HMTA concentration. It is noteworthy to mention that overall there were no appreciable differences in color values and the films shows moderate red-yellow color or orangish color.

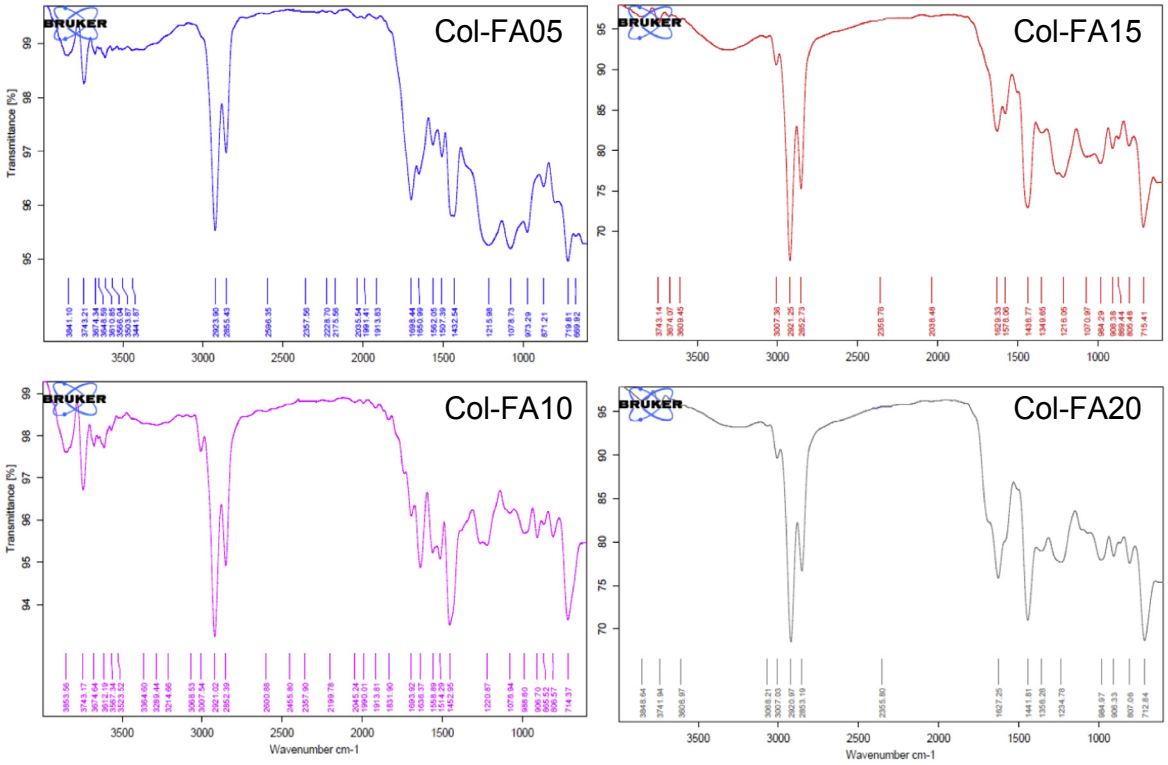

Fig. 5. ATR of Col-FA thin films.

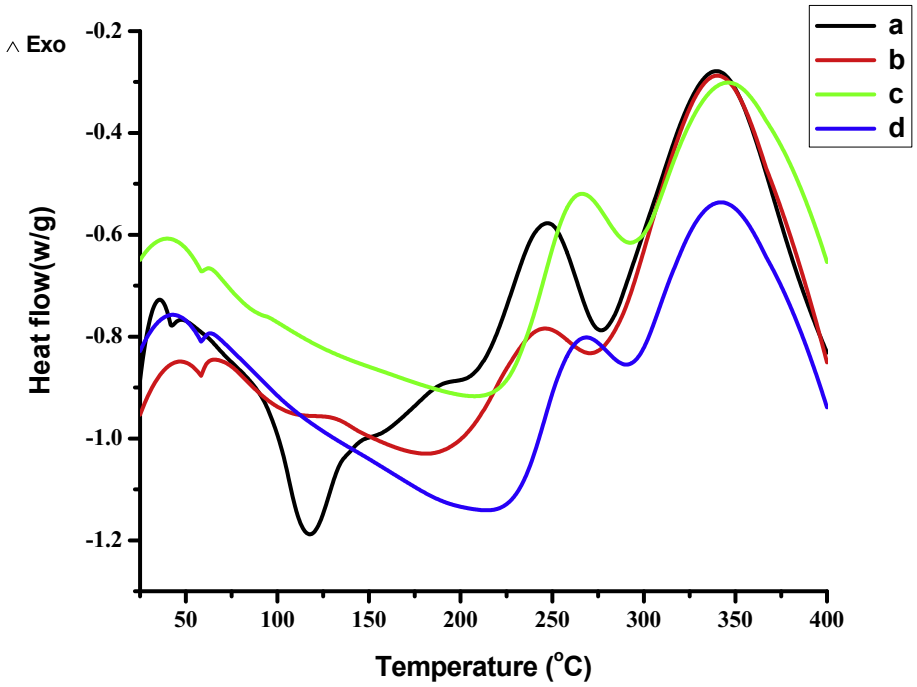

Fig. 6. DSC thermogram of (a) Col-FA05 (b) Col-FA10 (c) Col-FA15(d) Col-FA20 film.

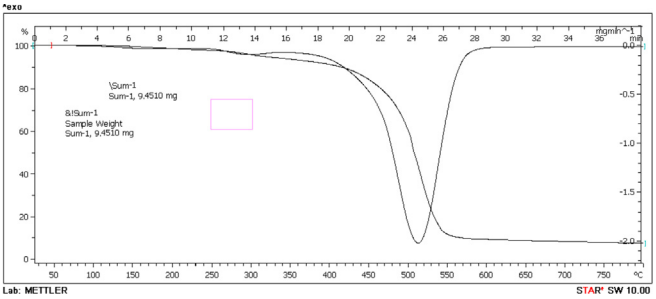

Fig. 7.1. TGA/DTA thermogram of Col-FA05 film.

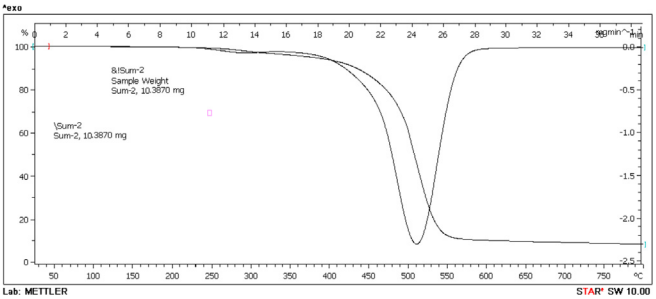

Fig. 7.2. TGA/DTA thermogram of Col-FA10 film.

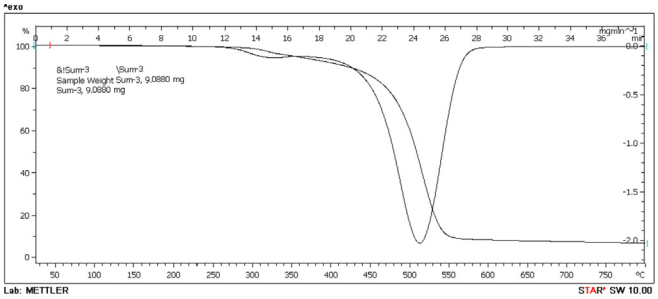

Fig. 7.3. TGA/DTA thermogram of Col-FA15 film.

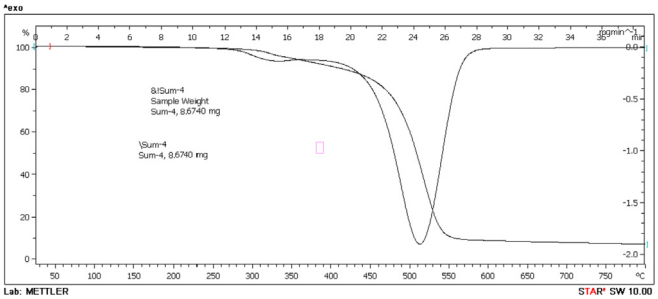

Fig. 7.4. TGA/DTA thermogram of Col-FA20 film.

3.7. *Physico-mechanical properties*

The physico-mechanical properties of all the compositions of Col-FA coated CS are presented in Table 5. The results indicated that the gloss values of the Col-FA compositions were enhanced with the increase in % HMTA concentration with maximum gloss shown by Col-FA15. The increased gloss value can be attributed to the increase in cross-link density with increasing concentration of HMTA, which, in turn, reflects large amount of light and resulted in high gloss value. Similarly, the scratch hardness value increased from Col-FA05 to Col-FA15 can also be correlated to the effective cross-linked network and improved adhesion between Col-FA and CS (Pathan and Ahmad, 2013). The cross-hatch adhesion results of all compositions further supports the good adhesion of coating material on CS. All the coatings except Col-FA20 passed 150 lb/in. impact resistance test and 1/8 in. conical mandrel bend test. The

Table 3
Thickness and opacity of Col-FA films.

Films	Thickness (mm)	Opacity (Abs_{650}/mm)
Col-FA05	0.11	3.03
Col-FA10	0.12	4.18
Col-FA15	0.18	2.83
Col-FA20	0.13	3.15

Table 4
Color values of the Col-FA films.

Films	L^*	a^*	b^*	C^*	h	ΔE_{cmc}
Col-FA10	25.87	4.76	1.77	5.08	20.43	24.26
Col-FA15	23.49	4.15	1.79	4.52	23.39	24.83
Col-FA20	26.28	3.59	0.72	3.66	11.28	23.71

Table 5
Physico-mechanical properties of all the compositions of Col-FA.

Properties	Sample code			
	Col-FA05	Col-FA10	Col-FA15	Col-FA20
Scratch Hardness(kg)	1.7	1.9	2.0	1.8
Cross hatch adhesion (%)	95	100	100	90
Impact Resistance (150 lb/inch)	Pass	Pass	Pass	Fail
Bend test (1/8 inch)	Pass	Pass	Pass	Fail
Gloss at 45°	74	76	80	70

bend test revealed that the coatings were flexible (except Col-FA20), as they could be bent without any damage or fracture (Fig. 4d). The flexibility in the coating is due to the presence of aliphatic hydrocarbon chain in the Col moiety that offers a plasticizing effect in the coating (De and Karak, 2013). The overall physico-mechanical test results indicated Col-FA15 composition to be the best for coating application.

3.8. Thermogravimetric analysis

The TGA/DTA curves of Col-FA thin films of different compositions were represented in Fig. 7.1 to 7.4 while the thermal data such as initial decomposition temperature (IDT) and temperature at 10% weight (T_{10}) loss along with IPDT data were tabulated in Table 6. It was revealed that IDT of Col-FA increases with HMTA up to Col-FA15 whereas 10 wt % loss was observed in the temperature range 422–450 °C. In addition to this, the thermal stability will decrease if more than 15% HMTA is used as this percentage is more than enough to react with all the available functional sites (Alaminov et al., 1976). Thus, the amount of HMTA used in the modification of Col-F tends to affect the thermal stability pattern.

TGA/DTA thermogram (Fig. 7.1 to 7.4) of all the compositions of Col-FA followed almost the same degradation pattern. It proceeds through two degradation steps in which slight degradation was observed in the first step and maximum degradation at second step. The first degradation step revealed as an small and broad endothermic peak in the DTA thermogram of all the compositions with a peak maxima in the range of 300–320 °C, can be correlated to the opening of benzoxazine rings and polymerization followed by the crosslinking of the polymeric chain with the expel of ammonia as a byproduct (Connor et al., 1987). The difference in thermal properties of Col-FA films was observed in this range. The second steep weight loss ranging from 450 to 560 °C which can clearly seen as a sharp endothermic peak with peak maxima at about 510–515 °C (as shown in DTA thermogram) in nearly all compositions corresponds to the scission of the methylene linkages in the long alkyl chain. This degradation step was similar in all the composition of Col-FA films. The steep decline in weight at second stage can be correlated to the length of alkyl chain, the longer the length of alkyl chain, the steeper will be the decline in weight loss (Connor et al., 1987).

In addition to this, the overall thermal stability of all the compositions, i.e., Col-FA05, Col-FA10, Col-FA15, and Col-FA20 can be determined by calculating IPDT values. Comparing the thermograms of all compositions revealed the inherent thermal stability to be in the range of 540 °C −550 °C.

3.9. Morphology of Col-FA thin film

3.9.1. XRD

The XRD pattern was shown in Fig. 8. It reveals that the composition of Col-FA15 thin film seems to be amorphous in nature as indicated by the appearance of a broad hump at 2θ value of 20–22°.

3.9.2. FE-SEM micrographs

FE-SEM micrographs of fractured surface of Col-FA15 thin film were shown in Fig. 9 at different magnifications. The micrographs revealed that Col-FA15 film surface seems to be dense, rough, and homogenous composed of spherical nanostructures that can be formed by thermally activated chemical reaction of Col-FA.

3.10. Chemical resistance of Col-FA thin film

Fig. 10 shows the comparative acids (3.5% HCl), alkalis (3.5% NaOH), salt (3.5% NaCl) and water resistance of Col-FA thin films of various compositions for 30 days. This clearly illustrates that out of all the films prepared from various compositions, Col-FA15 offered better resistance towards aforementioned concentration of acid, alkalis, salt as well as water. All the compositions except Col-FA15 showed maximum weight loss within a period of 30 days in acid (3.5% HCl), alkali (3.5% NaOH) and salt (3.5% NaCl). The maximum resistance offered by Col-FA15 can be attributed to the fact that while increasing the percentage of HMTA from 5% to 15%, the extent of crosslinking tend to increase resulting in a highly cross-linked structure of Col-FA15 composition. The water resistance of all of the compositions showed minimum weight loss and homogeneity after 1 month of dipping. This could be attributed to the hydrophobic nature due to the long alkyl chain of Col moiety, thereby, resisting any probable interaction between crosslinked structure and water. Hence, the chemical resistance test revealed Col-FA15 to be the best composition in our case.

Table 6
Thermal analysis data of Col-FA films.

Code	IDT (°C)	T_{10} (°C)	T_i (°C)	T_f (°C)	S_1	S_2	S_3	A^*	K^*	IPDT (°C)
Col-FA05	270	425	25	800	39760.44	5665.25	32075.86	0.59	1.14	543.97
Col-FA10	312	450	25	800	39637.19	6326.16	31536.66	0.593	1.15	557.99
Col-FA15	330	445	25	800	41106.14	4919.79	31474.84	0.594	1.12	540.34
Col-FA20	310	422	25	800	40675.73	5194.86	31631.74	0.592	1.13	542.27

T_{10}: Temperature at 10% weight loss.

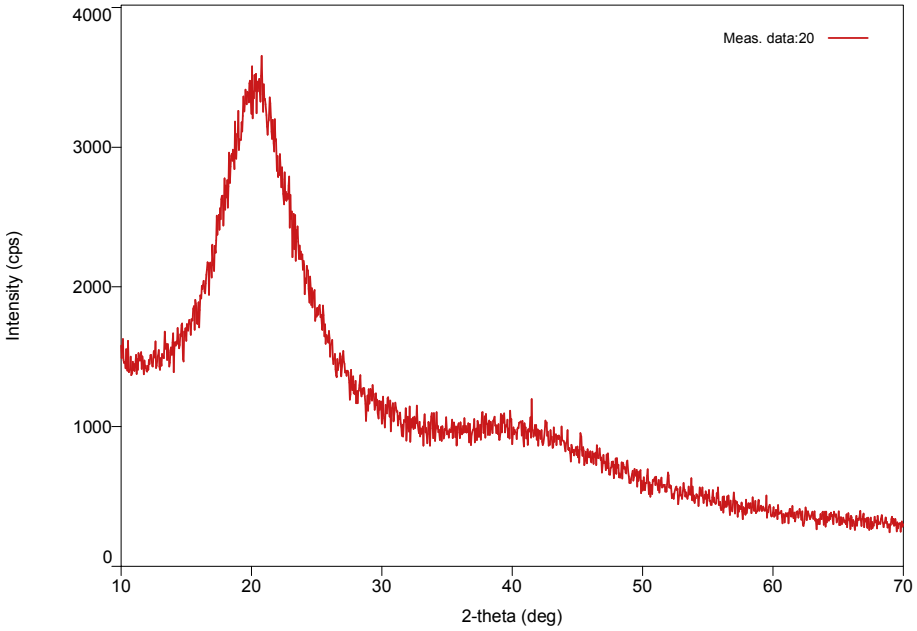

Fig. 8. XRD micrograph of Col-FA15 thin film.

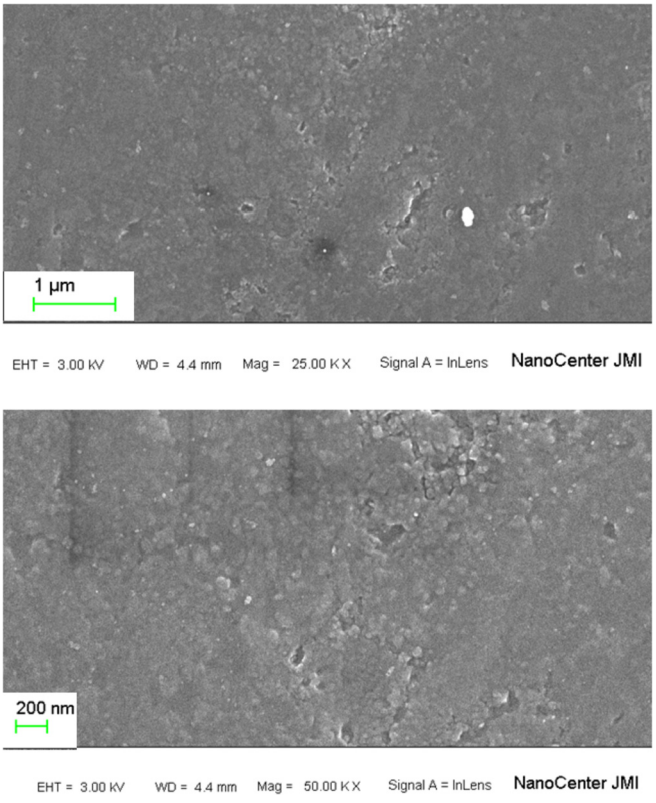

Fig. 9. SEM photograph of the fractured surface of Col-FA15 thin film at different magnifications.

3.11. Antibacterial activity

The antibacterial activity of Col, Col-F and Col-FA15 resin was carried out using Disk diffusion method. Results of antibacterial studies were given in Table 7, which revealed moderate antibacterial activity observed in the form of zone of growth inhibition (Fig. 11). Among the three concentrations tested, the least concentration (i.e. 62.50 µg/ml) showed clear zone of inhibition for *E. coli*, *S. aureus* and *B. subtilis*, but had no effect on *P. aerugenosa.* Higher concentrations showed a smaller zone of inhibition probably due to solubility issues with aqueous medium. Almost similar antibacterial activity against all strains was observed for Col and Col-FA15.

The antibacterial activity of Col (a phenolic lipid) could be attributed to its amphiphilic nature that allow the interactions with cellular membranous structures and hydrophobic domains of proteins present in bacterial cell wall (Stasiuk and Kozubek, 2010). Col showed maximum antibacterial activity against *E. coli* with zone of inhibition diameter of 11 mm. However, the antibacterial activity of Col-F is somewhat less as compared to Col that may be attributed to high molecular weight of the former resulting in lesser diffusion of compound. Further, there is slight improvement in the antibacterial efficacy in Col-FA15 in comparison to Col-F but not to a great extent that might be correlated to the benzoxazine ring structure containing N-alkylated group that are generally less active as compared to free −NH groups (Alper-Hayta et al., 2006). Although the antibacterial activity of Col-FA15 is not comparable to the standard antibiotic drug, i.e. Ampicillin, yet it is moderate enough to develop antibacterial films/coatings to be used in medical devices.

4. Conclusion

This paper introduces an innovative, widely applicable, straightforward, rapid, inexpensive and environment friendly method to prepare free standing, transparent, flexible Col-FA thin films/coatings via following simple and cleaner route. The synthesis of Col-FA in five different compositions were carried out and the mechanism involved in the same is discussed with the aid of FTIR, ^{1}H-NMR and ^{13}C-NMR spectral techniques. The thin film formation was first time analyzed by ATR-FTIR and DSC. The films obtained were transparent, flexible and falls under the category of reddish-yellow zone as confirmed through color analysis of films. The physico-mechanical analysis also confirmed the improved mechanical strength with good adhesion, bending ability (1/8 inch bend test), impact resistant (150 lb/inch), scratch resistant (2 kg)

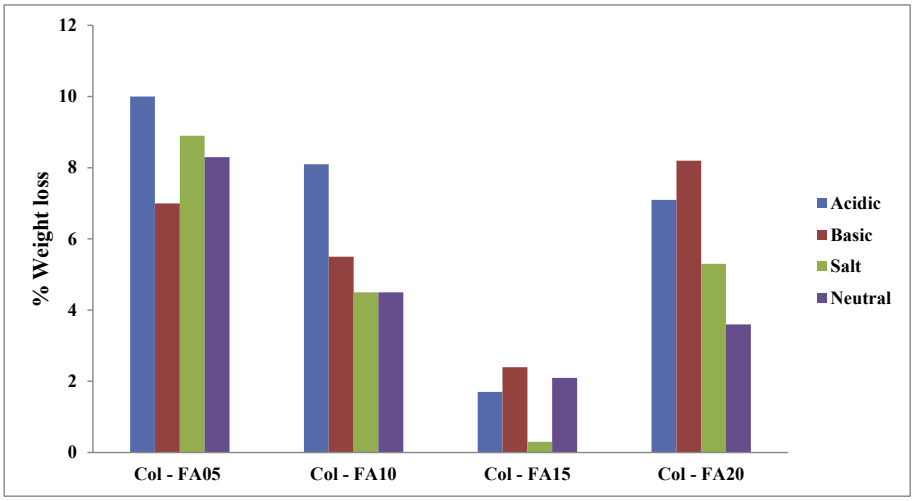

Fig. 10. Percent weight loss of Col-FA film in different chemical environments.

Table 7
Antibacterial activity results.

Zone of inhibition(mm)				
Abbreviation	*E.coli*	*S.aureus*	*B. substilis*	*P.aeruginosa*
Col	11	8	7	0
Col-F	9	0	7	0
Col-FA15	11	7	7	0
Ampicillin	28	27	35	15

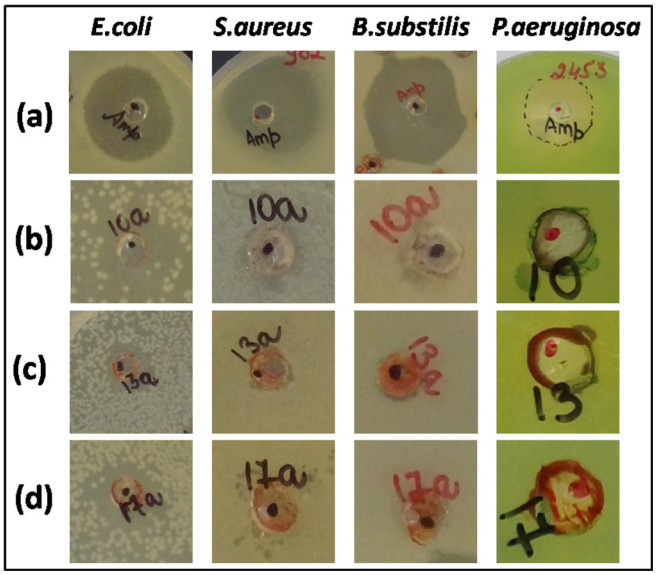

Fig. 11. Comparison of inhibition zone against different bacterial strains for (a) Ampicillin, standard drug (b) Col (c) Col-F (d) Col-FA15.

with excellent gloss values (80°). Overall, among all the synthesized compositions, Col-FA15 turned out to be the best composition in the present case having dense, homogeneous and amorphous morphology, excellent chemical resistance (against various solvents), thermally stable (up to 430–440 °C) with moderate antibacterial activity against *E. coli, S. aureus and B. subtilis*.

In a nutshell, this cost-effective and cleaner approach can be utilized for the synthesis of Col-FA that could be employed as an environment friendly, green material for versatile applications in the field of packaging, antimicrobial films and coatings in numerous medical devices. Certain limitations such as water insolubility, high temperature curing of the material will be improved in future work. The synthesis of coordination polymers (CPs) of Col-FA will be carried out to enhance the moderate antibacterial activity of the material that may find further applications in the biomedical field. Other improvement in functional aspects for broader applications is highly desirable in the near future.

Acknowledgements

Shabnam Khan wish to acknowledge University Grants Commission (UGC), New Delhi, India for financial support as SRF (Ref #F1-17.1/2014-15/MANF-2014-15-MUS-UTT-36965/(SA-III/Website). Dr Fahmina Zafar is thankful to UGC for Dr. D. S. Kothari postdoctoral fellowship [Ref. #F.4/2006(BSR)/13–986/2013(BSR), 2013–2016] and the Department of Science & Technology, New Delhi, India for the award of fellowship under the Women Scientists Scheme (WOS) for Research in Basic/Applied Sciences (Ref. No. SR/WOS-A/CS-97/2016). Authors are thankful to the Head, Department of Chemistry, Jamia Millia Islamia (JMI), for providing facilities to carry out the research work. Authors are also thankful to Centre for Nanoscience and Nanotechnology, JMI for FE-SEM analysis and Centre Instrumentation facilities (CIF), Centre for Interdisciplinary Research in Basic Sciences, JMI, for ATR, XRD and UV–Visible Spectrophotometer for opacity analysis. Authors also wish to acknowledge Dr. Shahid-ul-Islam, Postdoc fellow at Department of Textile Technology, Indian Institute of Technology (IIT), Delhi for carrying out the color analysis of films.

References

Alaminov, H., Markova, R., Slavova, S., 1976. Investigation on curing and destruction of crosslinked modified phenolformaldehyde polymers. J. Appl. Polym. Sci. 20, 1533–1541.
Alper-Hayta, S., Aki-Sener, E., Tekiner-Gulbas, B., Yildiz, I., Temiz-Arpaci, O., Yalcin, I., Altanlar, N., 2006. Synthesis, antimicrobial activity and QSARs of new benzoxazine-3-ones. Eur. J. Med. Chem. 41, 1398–1404.
Anastas, P.T., Warner, J.C., 1998. Green chemistry: theory and practice. Oxford University, New York, p. 30.
Balgude, D., Sabnis, A., Ghosh, S., 2016. Synthesis and characterization of cardanol based aqueous 2K polyurethane coatings. Eur. Polym. J. 85, 620–634.
Balgude, D., Sabnis, A., Ghosh, S., 2017a. Synthesis and characterization of cardanol based reactive polyamide for epoxy coating application. Prog. Org. Coating 104, 250–262.
Balgude, D., Sabnis, A., Ghosh, S., 2017b. Designing of cardanol based polyol and its

curing kinetics with melamine formaldehyde resin. Des. Monomers Polym. 20, 177–189.
Calo, E., Maffezzoli, A., Mele, G., Martina, F., Mazzetto, S.E., Tarzia, A., Stifani, C., 2007. Synthesis of a novel cardanol-based benzoxazine monomer and environmentally sustainable production of polymers and bio-composites. Green Chem. 9, 754–759.
Chuayjuljit, S., Rattanametangkool, P., Potiyaraj, P., 2007. Preparation of cardanol–formaldehyde resins from cashew nut shell liquid for the reinforcement of natural rubber. J. Appl. Polym. Sci. 104, 1997–2002.
Connor, D.O., Blum, F.D., 1987. Thermal Stability of Substituted Phenol-formaldehyde Resins, vol. 33, pp. 1933–1941.
De, B., Karak, N., 2013. Novel high performance tough hyperbranched epoxy by an A 2+ B 3 polycondensation reaction. J. Mater. Chem. A. 1 (2), 348–353.
De Medeiros, E.S., Agnelli, J.A.M., Joseph, K., De Carvalho, L.H., Mattoso, L.H.C., 2003. Curing behavior of a novolac-type phenolic resin analyzed by differential scanning calorimetry. J. Appl. Polym. Sci. 90, 1678–1682.
Doyle, C.D., 1961. Estimating thermal stability of experimental polymers by empirical thermogravimetric analysis. Anal. Chem. 33, 77–79.
Feng, J., Zhao, H., Yue, S., Liu, S., 2017. One-Pot synthesis of cardanol-derived high-efficiency antioxidants based on intramolecular synergism. ACS Sustain. Chem. Eng. 5, 3399–3408.
García, B.B., Liu, D., Sepehri, S., Stephanie, C., Beckham, D.M., Savage, L.W., Cao, G., 2010. Hexamethylenetetramine multiple catalysis as a porosity and pore size modifier in carbon cryogels. J. Non-Cryst. Solids 356, 1620–1625.
Gopalakrishnan, S., Nevaditha, N.T., Mythili, C.V., 2011. Antibacterial activity of azo compounds synthesized from the natural renewable source. Cardanol. J. Chem. Pharmaceut. Res. 3, 490–497.
Greco, A., Brunetti, D., Renna, G., Mele, G., Maffezzoli, A., 2010. Plasticizer for poly(vinyl chloride) from cardanol as a renewable resource material. Polym. Degrad. Stabil. 95, 2169–2174.
Greco, A., Maffezzoli, A., 2016. Cardanol derivatives as innovative bio-plasticizers for poly(lactic acid). Polym. Degrad. Stabil. 132, 213–219.
Greco, A., Ferrari, F., Maffezzoli, A., 2017. UV and thermal stability of soft PVC plasticized with cardanol derivatives. J. Clean. Prod. 164, 757–764.
Ishida, H., Ohba, S., 2005. Synthesis and characterization of maleimide and norbornene functionalized benzoxazines. Polymer 46, 5588–5595.
Khan, S., Laxmi, Zafar, H., Sharmin, E., Zafar, F., Nishat, N., 2016a. Cashew nut shell liquid based advanced functional materials. In: Padinjakkara, A., Thankappan, A., Gomes, F., Thomas, S. (Eds.), Biopolymers and Biomaterials. Apple Academic Press Inc., USA, ISBN 9781315161983.
Khan, S., Laxmi, Zafar, F., Nishat, N., 2016b. Development of bio-derived nano-structured coordination polymers based on cardanol-formaldehyde polyurethanes with "d^5" Mn(II) and "d^{10}" Zn(II) metal nodes: synthesis, characterization and adsorption behavior. RSC Adv. 6, 50070–50082.
Knop, V.A., Pilato, L.A., 1985. Phenolic resins. Chemistry, applications and performance, future directions. Springer-Verlag, New York.
Lalitha, K., Prasad, Y.S., Maheswari, C.U., Sridharan, V., John, G., Nagarajan, S., 2015. Stimuli responsive hydrogels derived from a renewable resource: synthesis, self-assembly in water and application in drug delivery. J. Mater. Chem. B. 3, 5560–5568.
Laxmi, Khan, S., Kareem, A., Zafar, F., Nishat, N., 2018. Synthesis, vibrational spectrometry and thermal characterizations of coordination polymers derived from divalent metal ions and hydroxyl terminated polyurethane as ligand. Spectrochim. Acta Part A Mol. Biomol. Spectrosc. 188, 400–410.
Liang, B., Li, X., Hu, L., Bo, C., Zhou, J., Zhou, Y., 2016. Foaming resol resin modified with polyhydroxylated cardanol and its application to phenolic foams. Ind. Crop. Prod. 80, 194–196.
Li, S., Yan, S., 2015. Synthesis and characterization of novel biobased benzoxazines from cardbisphenol and the properties of their polymers. RSC Adv. 5, 61808–61814.
Lochab, B., Varma, I.K., 2012. Cardanol-based bisbenzoxazines: effect of structure on thermal behaviour. J. Therm. Anal. Calorim. 107, 661–668.
Manjula, S., Pavithran, C., Pillai, C.K.S., Kumar, V.G., 1991. Synthesis and mechanical properties of cardanol-formaldehyde (CF) Resins and CF- poly(-methylmethacrylate) semi-interpenetrating polymer networks. J. Mater. Sci. 29, 4001–4007.
Martins, J.T., Cerqueira, M.A., Vicente, A.A., 2012. Influence of α-tocopherol on physicochemical properties of chitosan-based films. Food Hydrocolloids 27 (1), 220–227.
More, A.S., Sane, P.S., Patil, A.S., Wadgaonkar, P.P., 2010. Synthesis and characterization of aromatic polyazomethines bearing pendant pentadecyl chains. Polym. Degrad. Stabil. 95, 1727–1735.
Natarajan, M., Murugavel, S., 2013. Synthesis, spectral and thermal degradation kinetics of novolac resins derived from cardanol. High Perform. Polym. 25, 685–696.
Pathak, S.K., Rao, B.S., 2006. Structural effect of phenalkamines on adhesive viscoelastic and thermal properties of epoxy networks. J. Appl. Polym. Sci. 102, 4741–4748.
Pathan, S., Ahmad, S., 2013. Synthesis, characterization and the effect of the s-triazine ring on physico-mechanical and electrochemical corrosion resistance performance of waterborne castor oil alkyd. J. Mater. Chem. A. 1 (45), 14227–14238.
Peng, Y., Wu, Y., Li, Y., 2013. Development of tea extracts and chitosan composite films for active packaging materials. Int. J. Biol. Macromol. 59, 282–289.
Puchot, L., Verge, P., Fouquet, T., Vancaeyzeele, C., Vidal, F., Habibi, Y., 2016. Breaking the symmetry of dibenzoxazines: a paradigm to tailor the design of bio-based thermosets. Green Chem. 18 (11), 3346–3353.
Raj, C.I.S., Christudhas, M., Raj, G.A.G., 2011. Synthesis, characterization, metal ion intake and antibacterial activity of cardanol based polymeric schiff base transition metal complexes using ethylenediamine. J. Chem. Pharmaceut. Res. 3, 127–135.
Rao, B.S., Palanisamy, A., 2011. Monofunctional benzoxazine from cardanol for bio-composite applications. React. Funct. Polym. 71, 148–154.
Rather, L.J., Shahid, M., Khan, M.A., Mohammad, F., 2014. Study the effect of ammonia post-treatment on color characteristics of annatto-dyed textile substrate using reflectance spectrophotometery. Ind. Crop. Prod. 59, 337–342.
Ravichandran, S., Bouldin, R.M., Kumar, J., Nagarajan, R., 2011. A renewable waste material for the synthesis of a novel non-halogenated flame retardant polymer. J. Clean. Prod. 19 (5), 454–458.
Sharmin, E., Zafar, F., Nishat, N., Ahmad, S., 2016. Recent advances in environment friendly alkyd nanocomposites towards "greener" coatings. In: Larramendy, M., Soloneski, S. (Eds.), Green Nanotechnology – Overview and Further Prospects. InTech Open access publishers, pp. 193–207.
Shukla, S., Mahata, A., Pathak, B., Lochab, B., Nagar, G.B., 2015. Cardanol benzoxazines – interplay of oxazine functionality (mono to tetra) and properties. RSC Adv. 5, 3–9.
Silverstein, R.M., Bassler, G.C., Morrill, T.C., 1991. Spectrometric identification of organic compounds, fifth ed. Wiley, New York.
Srivastava, R., Srivastava, D., 2013. Utilization of renewable resources in the synthesis of novolac polymers: studies on its structural and curing characteristics. Int. J. Res. Rev. Eng. Sci. Technol. 2, 22–25.
Stasiuk, M., Kozubek, A., 2010. Biological activity of phenolic lipids. Cell. Mol. Life Sci. 67, 841–860.
Vaithilingam, S., Jayanthi, K.P., Muthukaruppan, A., 2017. Synthesis and characterization of cardanol based fluorescent composite for optoelectronic and antimicrobial applications. Polymer 108, 449–461.
Velez-Herrera, P., Ishida, H., 2009. Low temperature polymerization of novel, monotropic liquid crystalline benzoxazines. J. Polym. Sci. Part A Polym. Chem. 47, 5871–5881.
Vyazovkin, S., Sbirrazzuoli, N., 2006. Isoconversional kinetic analysis of thermally stimulated processes in polymers. Macromol. Rapid Commun. 27, 1515–1532.
Wang, L., Wang, Q., Tong, J., Zhou, J., 2017. Physicochemical properties of chitosan films incorporated with honeysuckle flower extract for active food packaging. J. Food Process. Eng. 40, 1–8.
Wang, X., Kalali, E.N., Wang, D.-Y., 2015a. Renewable cardanol-based surfactant modified layered double hydroxide as a flame retardant for epoxy resin. ACS Sustain. Chem. Eng. 3, 3281–3290.
Wang, Y., Wang, S., Bian, C., Zhong, Y., Jing, X., 2015b. Effect of chemical structure and cross-link density on the heat resistance of phenolic resin. Polym. Degrad. Stabil. 111, 239–246.
Wazarkar, K., Kathalewar, M., Sabnis, A., 2017. High performance polyurea coatings based on cardanol. Prog. Org. Coating 106, 96–110.
Yadav, R., Srivastava, D., 2009. Synthesis and properties of cardanol-based epoxidized novolac resins modified with carboxyl-terminated butadiene–acrylonitrile copolymer. J. Appl. Polym. Sci. 114, 1670–1681.
Yadav, M., Sand, A., Behari, K., 2012. Synthesis and properties of a water soluble graft (chitosan-g-2-acrylamidoglycolic acid) copolymer. Int. J. Biol. Macromol. 50, 1306–1314.
Zafar, F., Azam, M., Sharmin, E., Zafar, H., Haq, Q.M.R., Nishat, N., 2016. Nano-structured coordination complexes/polymers derived from cardanol: "one-pot, two-step" solventless synthesis and characterization. RSC Adv. 6, 6607–6622.
Zhang, X., Solomon, D.H., 1998. The chemistry of novolac resins: reaction pathways studied via model systems of ortho-hydroxybenzylamine intermediates and phenols. Polymer 39, 6153–6162.